Synthesis of Poly(methacrylic acid) Brushes via Surface-Initiated Atom Transfer Radical Polymerization of Sodium Methacrylate and Their Use as Substrates for the Mineralization of Calcium Carbonate

Stefano Tugulu,[†] Raphaël Barbey,[†] Marc Harms,[‡] Marc Fricke,[‡] Dirk Volkmer,*[,‡] Antonella Rossi,[§,||] and Harm-Anton Klok*[,†]

École Polytechnique Fédérale de Lausanne (EPFL), Institut des Matériaux, Laboratoire des Polymères, Bâtiment MXD, Station 12, CH-1015 Lausanne, Switzerland, University of Ulm, Anorganische Chemie II, Albert-Einstein-Allee 11, D-89081 Ulm, Germany, Swiss Federal Institute of Technology (ETHZ), Department of Materials, Laboratory for Surface Science and Technology, Wolfgang-Pauli-Strasse 10, ETH Hönggerberg, CH-8093 Zürich, Switzerland, and Università degli Studi di Cagliari, Dipartimento di Chimica Inorganica ed Analitica, I-09100 Cagliari, Sardinia, Italy

Received April 2, 2006; Revised Manuscript Received September 21, 2006

ABSTRACT: This manuscript describes the synthesis of poly(methacrylic acid) (PMAA) brushes via surface-initiated atom transfer radical polymerization (SI-ATRP) of sodium methacrylate (NaMA) and their use as substrates for the mineralization of calcium carbonate. A $CuBr/CuBr_2$/bipyridine catalyst system in aqueous solution at room temperature allowed the synthesis of brushes with thicknesses of up to 300 nm. Using substrates modified with mixtures of an ATRP-initiator modified trimethoxysilane and an "inert" pivaloyl-modified trimethoxysilane to initiate the ATRP of NaMA, a series of brushes with varying chain density could be prepared. Subsequent mineralization experiments revealed that, while low-density brushes promoted the formation of calcite crystals, high-density brushes were covered with a thin layer of amorphous $CaCO_3$ (ACC). This is of interest because ACC can serve as a metastable precursor for different crystalline $CaCO_3$ polymorphs and offers attractive perspectives for the bottom-up fabrication of well-defined $CaCO_3$ crystal architectures.

Introduction

Surface-initiated, controlled/"living" polymerization techniques are attractive tools to modify materials surfaces because the composition, thickness, and density of the resulting polymer layers ("brushes") can be controlled on the molecular level.[1−4] Brushes based on poly(ethylene glycol) methacrylate, for example, have been successfully used to suppress nonspecific protein adsorption.[5−8] Brushes generated from thermosensitive polymers that show lower critical solution temperature (LCST) behavior have been used for the programmed adsorption and release of proteins.[9] Polymer brushes have also been used for the synthesis of metal nanoparticles,[10] as templates for biomimetic silicification,[11] or as biolubricants.[12]

Polyelectrolyte brushes in particular have attracted considerable theoretical and experimental interest.[13−16] Polyelectrolyte brushes can change from an extended conformation in solutions of low ionic strength to a coiled conformation in solutions of high ionic strength and have therefore been proposed as nanoactuators.[17] In biology, acidic matrix macromolecules are involved in the production of sophisticated and well-defined calcified tissues such as bone or nacre.[18,19] Polyelectrolyte brushes exposing a multitude of acidic groups, therefore, may also be attractive tools to study and direct nucleation, morphology, and orientation of biologically relevant minerals. So far, molecularly well-defined substrates that have been used to study and direct growth of $CaCO_3$, the most abundant biomineral, include acid-functionalized self-assembled monolayers of alkanethiols on gold,[20,21] Langmuir monolayers of acidic surfactants,[22] as well as polymeric Langmuir−Schaefer films of acidic polydiacetylenes.[23] Other approaches that have been explored include the use of immobilized organic/polymer films such as poly(acrylic acid)/chitosan membranes,[24] poly(vinyl alcohol),[25] anionic starburst dendrimers,[26] collageneous matrices,[27] and organosilane-based thin films.[28] The last five examples, however, involved the use of deposition techniques that usually only provide limited means of controlling lateral dimensions, surface patterning, and thickness of the organic coating, which is required for advanced technical applications. Surface-initiated, controlled/"living" polymerization techniques are attractive tools to overcome these problems. To the best of our knowledge, however, negatively charged polyelectrolyte brushes prepared by surface-initiated atom transfer radical polymerization (SI-ATRP) have not yet been investigated as substrates to study and direct $CaCO_3$ mineralization.

Because the direct ATRP of (meth)acrylic acid may be hampered by reaction of the monomer with the metal complex to form catalytically ineffective metal carboxylates,[29,30] a number of authors has synthesized poly((meth)acrylic acid) brushes via SI-ATRP of *tert*-butyl(meth)acrylate, followed by hydrolysis or pyrolysis of the *tert*-butyl ester protective groups.[10,31,32] Apart from the fact that the deprotection of the *tert*-butyl group introduces an additional synthetic step, prolonged hydrolysis times were also found to result in partial cleavage of polymer chains from the surface.[10,33] Clearly, direct polymerization without the need for polymer analogous deprotection reactions is the more attractive approach. One possibility is to use sodium (meth)acrylate instead of (meth)acrylic acid. Billingham, Armes and co-workers were the first to report the direct ATRP of sodium methacrylate in aqueous media.[34] A modified version

* Authors to whom correspondence should be addressed. E-mail: harm-anton.klok@epfl.ch (H.-A.K.); dirk.volkmer@uni-ulm.de (D.V.).
[†] École Polytechnique Fédérale de Lausanne (EPFL).
[‡] University of Ulm, Anorganische Chemie II.
[§] Swiss Federal Institute of Technology (ETHZ).
[||] Università degli Studi di Cagliari, Dipartimento di Chimica Inorganica ed Analitica.

10.1021/ma060739e CCC: $37.00
Published on Web 12/24/2006

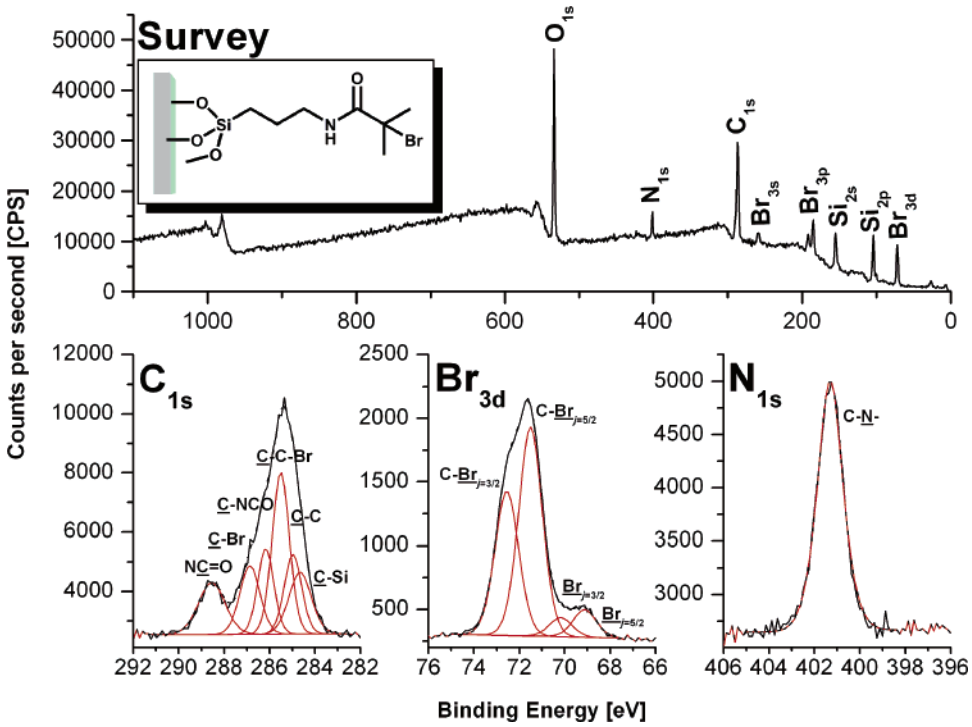

Figure 1. XPS survey spectrum and high-resolution elemental scans of the C_{1s}, Br_{3d}, and N_{1s} signals of an ATRP initiator **1** modified silicon substrate.

of their procedure was used by Huck et al. to grow polyelectrolyte brushes from gold-coated silicon surfaces.[35] These two studies, however, did not present an in-depth investigation of the polymerization kinetics and of the influence of reaction parameters such as temperature, pH, monomer concentration, and ion strength. This seems surprising because both the conventional aqueous free radical polymerization of methacrylic acid and the ATRP of sodium methacrylate in water are known to be sensitive to pH.[34]

Motivated by the possible use of poly((meth)acrylic acid) brushes as substrates to direct the growth of inorganic materials, we were interested in gaining a more thorough understanding of the parameters that govern the SI-ATRP of sodium methacrylate. In this paper, we will report the influence of temperature, pH, monomer concentration, and ion strength on the SI-ATRP of sodium methacrylate and we will describe first investigations on the use of the resulting brushes as substrates for the mineralization of calcium carbonate.

Experimental Section

Materials. Surface-initiated atom transfer radical polymerization (SI-ATRP) was performed on commercially available glass microscopy slides (Menzel Gläser, usually cut into 2 cm × 1 cm pieces) as well as on silicon wafers (2 cm × 0.8 cm) for ellipsometric measurements. For crystallization experiments, round glass cover slips (Hecht-Assistant, circular, 25 mm diameter) were used. Sodium methacrylate (NaMA) was obtained from Aldrich and used as received. Bipyridine (bipy) was obtained from Fluka and recrystallized twice from hexane. Deionized water was obtained from a Milli-Q Ultrapure water purification system. Toluene was dried over sodium. Dichloromethane was dried over phosphorus pentoxide. 2-Bromo-2-methyl-*N*-[3-(trimethoxysilyl)propyl]propanamide **1** and *N*-[3-(trimethoxysilyl)propyl]isobutyrylamide **2** were synthesized following a literature procedure[6] and purified by distillation under oil pump vacuum. All other reagents were obtained from commercial suppliers and used without further purification.

Analytical Methods. pH of reaction solutions were measured using a precalibrated pH electrode from Mettler Toledo. ATR-FTIR spectroscopy was performed on a nitrogen-purged Nicolet Magna-IR 560 spectrometer equipped with a Specac Golden Gate single-reflection diamond ATR system. Brush thicknesses were determined using a computer-controlled null ellipsometer (Phillips Plasmon SD 2300) working with a He−Ne laser ($\lambda = 632.8$ nm) and an angle of incidence of 70°. The method for calculation was based on a three-layer silicon/polymer brush/ambient model, assuming the polymer brush is isotropic and homogeneous. Refractive indices and thicknesses were calculated simultaneously from the experimental Ψ and Δ values. All reported ellipsometric film thicknesses are uncorrected for the 1−3 nm thick native oxide layer on the silicon substrates. As a result, the reported thicknesses of the ATRP initiator layers are higher than expected and the brush thicknesses slightly overestimated. Water contact angles were determined using a DataPhysics OCA 35 contact angle measurement system. Optical micrographs were recorded on a Olympus IX 70 microscope. XPS data were recorded on a Quantera SXM system from ULVAC-PHI (Figure 1, Figure 10) or on an Axis Ultra from Kratos Analytical (all other figures). The Quantera system was operated using a monochromatic Al Kα (1486.6 eV) source operating at 20.31 W with an X-ray beam diameter of 100 μm. The base pressure was 2×10^{-7} Pa and the instrument was calibrated according to the ISO 14572 standard procedure. High-resolution spectra were acquired applying a pass energy of 69 eV. The relative sensitivity factors (RSF) used for calculating the ratios of Figure 10 were obtained from Scofield's cross sections corrected for the instrumental geometry, transmission function and electron attenuation length. The values are 2.681 for N_{1s} and 5.479 for Br_{3d}.[36] Measurements with the Axis Ultra instrument from Kratos Analytical were carried out with a conventional hemispheric analyzer. The X-ray source employed was a monochromatic Al Kα (1486.6 eV) source operated at 150 W and 10^{-9} mbar. The analysis area was 700 × 350 μm at an angle of 90° relative to the substrate surface (take-off angle). The pass energies were 80 and 20 eV for wide scans and high resolution elemental scans, respectively. The operating software used was Vision 2, which corrects for the transmission function. Charge compensation was performed with a self-compensating device (Kratos patent) using field emitted low energy electrons (0.1 eV).

Scheme 1

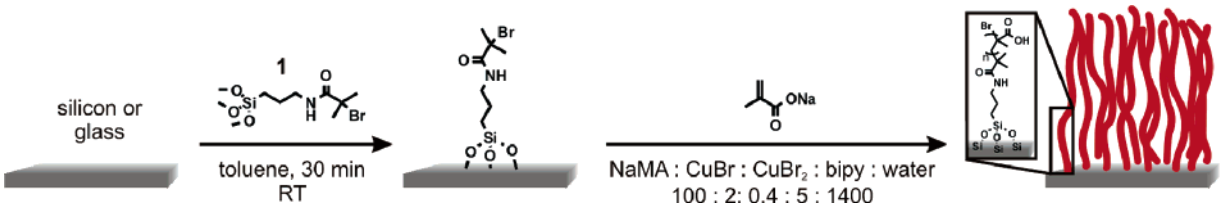

Surface Grafting of the ATRP Initiator. Glass and silicon substrates were sonicated in ethanol and in deionized water for 15 min. Subsequently, the slides were immersed in piranha solution (H_2SO_4/H_2O_2 (7:3; v:v)) for 30 min at 100−150 °C to remove any organic residues and to create silanol groups on the surfaces. The cleaned slides were rinsed extensively with water, ethanol, and dichloromethane and subsequently dried in a stream of nitrogen. Next, the slides were immersed in a 10 mM solution of **1** in anhydrous toluene for 30 min, washed with anhydrous toluene, sonicated in dichloromethane and acetone for 1 min, and dried in a stream of nitrogen. The substrates were directly used for SI-ATRP experiments.

General Procedure for the Surface-Initiated Atom Transfer Radical Polymerization of Sodium Methacrylate. Aqueous solutions of sodium methacrylate (NaMA) and bipyridine (bipy) were prepared by stirring at 50 °C until complete dissolution. After cooling to room temperature, the pH of the solutions was adjusted to the desired value by addition of 0.1 M aqueous solutions of HCl or NaOH. $CuBr_2$ was added and the solutions were degassed by applying two freeze−pump−thaw cycles. Next, CuBr was added and degassing was continued for two additional freeze−pump−thaw cycles. The reaction mixture was then transferred to nitrogen-purged reaction vessels containing the initiator-functionalized substrates. The reaction was allowed to proceed for a defined reaction time at a controlled temperature under nitrogen atmosphere. After that, the slides were thoroughly rinsed with water and extracted by washing 3 times for 2 h with water. The composition of the reaction mixture was based on the following molar ratios of monomer, catalyst and solvent: NaMA/CuBr/$CuBr_2$/bipy/water = 100:2:0.4:5:1400. In a typical experiment, the following amounts were used: 10.8 g (100 mmol) NaMA, 780 mg (5 mmol) bipy, 287 mg (2 mmol) CuBr, 90 mg (0.4 mmol) $CuBr_2$, and 25 mL (1.4 mol) water.

An additional experiment was carried out to evaluate the influence of ionic strength on the SI-ATRP of NaMA. In this case, sodium acetate (NaAc) was added to the reaction mixture, and the different reagents were used in the following molar ratios: NaMA/NaAc/CuBr/$CuBr_2$/bipy/water = 100:100:2:0.4:5:1400.

Synthesis of Poly(methacrylic acid)-*b*-poly(2-hydroxyethyl methacrylate) (PMAA-*b*-PHEMA) Brushes. First, a PMAA block was grown via SI-ATRP of NaMA on initiator-functionalized silicon wafers by applying a reaction mixture with molar ratios of NaMA/CuBr/$CuBr_2$/bipy/water = 200:2:0.4:5:1400 for 15 min at 25 °C. To quench the polymerization and to convert any reactive site into the corresponding dormant species, the polymerization solution was replaced by a degassed solution of 0.1 M bipy and 0.05 M $CuBr_2$. For the growth of the PHEMA block, this quenching solution was replaced by a degassed solution containing HEMA, CuCl, $CuBr_2$, bipy, and water in a 215:3.4:1:9.75:1430 molar ratio. The polymerization was allowed to proceed for 2.5 h at 25 °C under nitrogen atmosphere. The wafers were taken from the polymerization solution, washed with DMF, and subsequently extracted 3 times for 2 h with DMSO, rinsed with water, and dried in a stream of nitrogen.

Synthesis of Poly(2-hydroxyethyl methacrylate) (PHEMA) Brushes. SI-ATRP of HEMA was carried out as described in a previous report.[6]

Mineralization of Calcium Carbonate. Mineralization of calcium carbonate was carried out in a flow-through device as reported previously.[37] Briefly, round glass cover slips functionalized with a PMAA brush were mounted in a perfusion cell and exposed to a continuous flow of a supersaturated calcium carbonate solution for a defined time. The supersaturated calcium carbonate solution was prepared from a 10 mM $CaCl_2$ and a 10 mM Na_2CO_3 solution in a mixing chamber that was connected to the injection port of the perfusion cell. Solutions were injected into the mixing chamber at a flow rate of 0.75 mL/min. The substrates were subsequently rinsed with deionized water and dried at air.

Results and Discussion

Surface-Initiated Atom Transfer Radical Polymerization of Sodium Methacrylate. The synthesis of the poly(methacrylic acid) (PMAA) brushes is outlined in Scheme 1 and starts with the functionalization of a glass or silicon substrate with the ATRP initiator-functionalized trimethoxysilane **1**. The ATRP initiator-functionalized surfaces were characterized with contact angle measurements and XPS. Immobilization of the ATRP initiator **1** on an activated silicon substrate resulted in an increase in the advancing water contact angle from 0° to 81° and in the receding water contact angle from 0° to 42°. Figure 1 shows the XPS survey spectrum as well as high-resolution elemental scans of the C_{1s}, Br_{3d}, and N_{1s} signals, which were recorded from a silicon surface modified with **1**. In agreement with the elemental composition of **1**, the survey spectrum shows the appearance of a C_{1s} and N_{1s} as well as Br_{3p} and Br_{3d} signals. The C_{1s} signal can be fitted using six model Gaussian/Lorentzian curves with the expected peak area ratios. The components correspond to the six different types of carbon atoms that constitute **1**.

In a next step, the ATRP initiator-functionalized surfaces were used to investigate the polymerization of sodium methacrylate (NaMA). Surface-initiated atom transfer radical polymerization (SI-ATRP) of NaMA was carried out in aqueous solution using a CuBr/$CuBr_2$/bipy catalyst system. This reaction system is identical to that reported earlier by Huck et al.[35] In the present study, however, SI-ATRP is carried out on glass or silicon surfaces, whereas Huck and co-workers polymerized NaMA from gold-coated silicon surfaces modified with an ATRP initiator-functionalized thiol. In a first set of experiments, the polymerization conditions reported by Billingham, Armes et al.,[34] and Huck and co-workers[35] were evaluated using the following molar ratios of reagents/solvents: NaMA/CuBr/$CuBr_2$/bipy/water = 100:2:0.4:5:1400. Billingham, Armes, et al. have investigated the ATRP of NaMA at 90 °C in homogeneous aqueous solution and identified the optimum pH for the polymerization to be between 8 and 9. At pH values below 6, NaMA did not undergo ATRP because the bipy becomes protonated and no longer complexes $CuBr_2$.[34] Because of desorption of the ATRP initiator-functionalized thiols from the gold substrates, Huck et al. could not carry out the polymerization at 90 °C and prepared brushes at 60 °C, instead.[35] Figure 2 plots the ellipsometric film thickness versus polymerization time for the SI-ATRP of NaMA using the reaction system mentioned earlier at pH 8 and 9 and 60 °C and 90 °C. In contrast to Huck et al., who reported thicknesses of up to 60 nm, only layers of 4−7 nm were obtained. Changing the pH

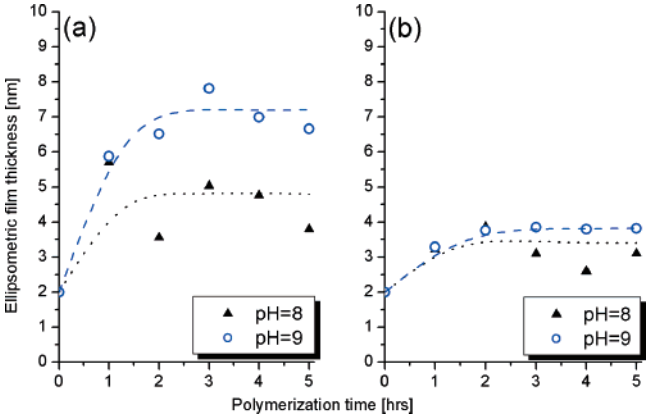

Figure 2. Evolution of film thickness as a function of polymerization time for the SI-ATRP of NaMA at (a) 60 and (b) 90 °C using a reaction system with the following composition: NaMA/CuBr/$CuBr_2$/bipy/water = 100:2:0.4:5:1400.

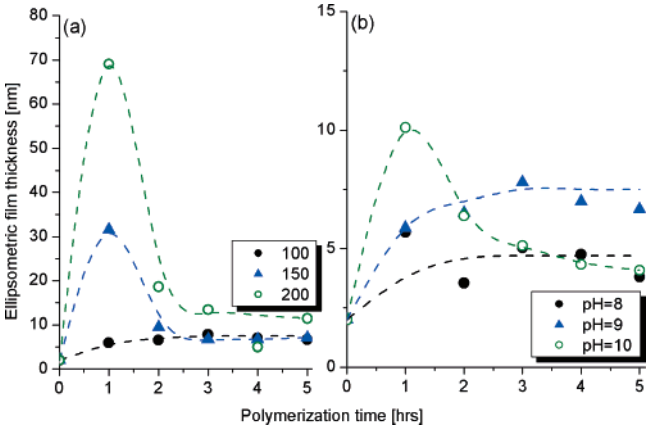

Figure 3. Effect of (a) monomer concentration and (b) pH on the SI-ATRP of NaMA at 60 °C. The variation of monomer concentration is carried out with a reaction system of the following composition: NaMA/CuBr/$CuBr_2$/bipy/water = 100/150/200:2:0.4:5:1400 at pH = 9. The effect of pH is analyzed using a reaction system with the following composition: NaMA/CuBr/$CuBr_2$/bipy/water = 100:2:0.4:5:1400.

from 8 to 9 or the reaction temperature from 60 °C to 90 °C did not significantly affect the brush thickness.

Monomer concentration was found to have a strong influence on the SI-ATRP of NaMA. Increasing the relative molar amount of NaMA from 100 to 150 to 200, while keeping the relative amounts of all other components of the reaction mixture constant, resulted in an increase in brush thickness after 1 h of polymerization time from 5 to 33 to 70 nm (Figure 3a). In addition to ellipsometry, the resulting brushes were characterized by means of contact angle measurements, ATR-FTIR spectroscopy, and XPS. Growth of the PMAA brushes resulted in a drop of the advancing water contact angle from 81° for the ATRP initiator modified surface to 32−55° for the PMAA brush. Although in all cases a clear drop in the advancing water contact angle was observed, the advancing water contact angles were found to be dependent on the polymerization conditions (i.e., monomer concentration, pH, temperature, and reaction time) that were used. As will be discussed in more detail below, these reaction parameters do not only influence the length of the tethered PMAA chains, but presumably also the chain density and, concomitantly, surface chemistry. The ATR-FTIR spectrum of the PMAA brush (Figure 8) revealed a carbonyl band at ~1702 cm^{-1}, which is characteristic for hydrogen-bonded dimers of carboxylic acid groups[38] and indicates that the brushes are composed of methacrylic acid (MAA) rather

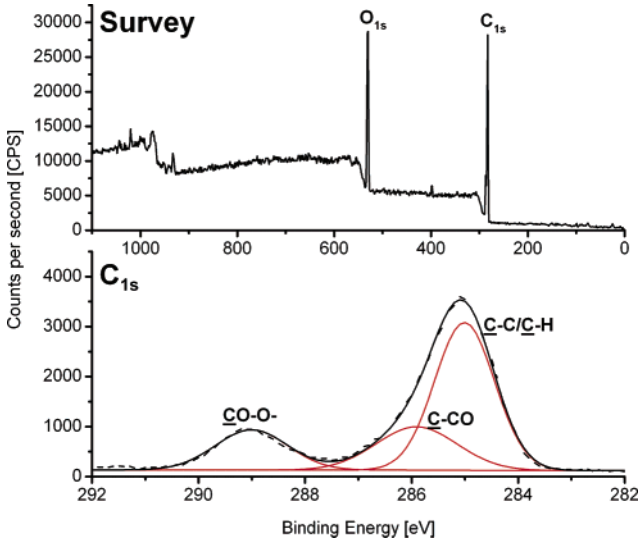

Figure 4. Survey and high-resolution scan of the C_{1s} signal of a ~100 nm thick PMAA brush supported on a silicon substrate.

than sodium methacrylate (NaMA). This is in agreement with earlier results by Huck et al., who attributed this to the water-washing step after the SI-ATRP and proposed that rinsing the brush surfaces with water would protonate the carboxylate groups and remove sodium ions from the polymer brush.[35] Figure 4 shows a XPS survey spectrum of a PMAA brush as well as a high-resolution scan of the C_{1s} signal. In agreement with the elemental composition of PMAA, the survey spectrum only shows carbon and oxygen signals. In the C_{1s} high-resolution scan, the carbon atom of the carboxy group can be clearly distinguished and is shifted about 4 to 288.5 eV relative to the aliphatic carbon atoms. Furthermore, the XPS survey spectrum does not reveal a sodium signal, which provides further evidence for the fact that the grafted polymer chains are composed of MAA rather than NaMA.

Figure 3a shows a significant decrease in ellipsometric film thickness after a polymerization time of 1 h at the two highest monomer concentrations. The observed decrease in film thickness is attributed to (partial) cleavage of the poly(methacrylic acid) (PMAA) chains from the surface. We assume that the high brush density leads to a stretched conformation of the polymer chains, which may "mechanically activate"[39] and facilitate hydrolysis of the siloxane bond that links the polymer chain to the surface. Similar observations have been made upon incubation of poly(poly(ethylene glycol) methacrylate) brushes, which were grafted from SiO_x surfaces, in cell culture media.[40] While polymerizations, which were carried out using 150 or 200 equiv NaMA, resulted in a decrease in film thickness with increasing polymerization time, no such phenomena were observed when the SI-ATRP was performed using 100 equiv NaMA. This makes it unlikely that the observed decrease is due to desorption of physically absorbed polymer because this would be expected to be independent of the relative monomer concentration. This is further supported by the observation that ultrasound treatment of ATRP initiator-modified substrates in order to remove any eventual physisorbed initiator species did not lead to different polymerization results. Furthermore, whereas PMAA brushes prepared at pH 8 or 9 were stable during the course of the polymerization, a decrease in film thickness was observed when the pH of polymerization was raised to pH 10 (Figure 3b). Because the hydrolysis of siloxane bonds is promoted under alkaline conditions, this supports the hypothesis that chain cleavage takes place at the siloxane bond that links the polymer chain to the surface.[41,42] A simple and sensitive method to probe

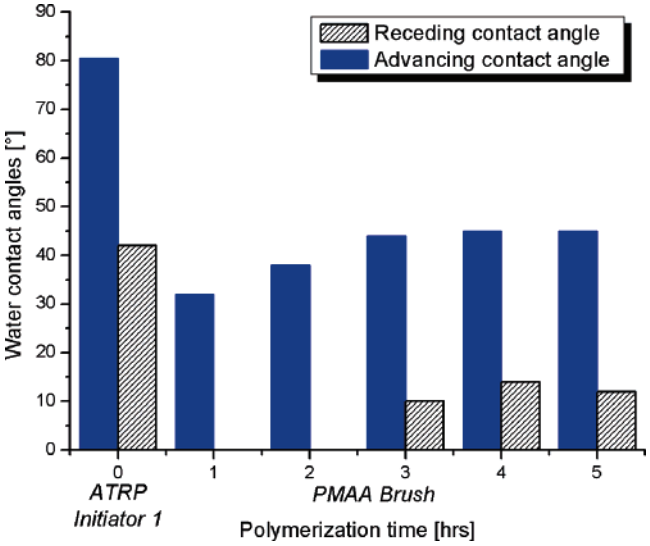

Figure 5. Water contact angles on PMAA brushes as a function of polymerization time for the SI-ATRP of NaMA at 60 °C using the following reaction system: NaMA/CuBr/$CuBr_2$/bipy/water = 100:2:0.4:5:1400, pH = 10.

the structural integrity and stability of polymer brushes is to measure water contact angles. Figure 5 shows the advancing and receding water contact angles on the PMAA brushes as a function of polymerization time. Comparison of Figures 3 and 5 reveals that the onset of the decrease in brush thickness correlates with an increase in the advancing and receding water contact angle. Interestingly, a similar increase in advancing and receding water contact angle was also observed upon analyzing a series of PMAA brushes with decreasing brush density (Figure 13). The origin of these observations is not clear at this moment and is the subject of ongoing investigations. Both cleavage of polymer chains from the surface and a decrease in brush density, however, are likely to influence the conformation of the surface-tethered polymer chains and may lead to different surface chemistry. Upon comparing Figure 13 and Figure 5, it should be kept in mind that the contact angles reported in Figure 13 were measured on brushes that were prepared at pH 9, whereas the contact angles shown in Figure 5 were determined on PMAA brushes synthesized at pH 10. This explains the difference between the water contact angle measured on the brush prepared with 100 mol % ATRP initiator **1** ($\chi_1^{solution}$) in Figure 13 and the values represented in Figure 5.

Next, it was attempted to modify the conditions of the SI-ATRP of NaMA at a monomer concentration of 200 mol equiv so as to prevent cleavage of PMAA chains during brush growth. Surprisingly, a considerable increase in film thickness could be achieved by decreasing the polymerization temperature from 60 to 25 °C (Figure 6). PMAA brushes with thicknesses of up to 300 nm could be prepared within 3 h at 25 °C. These brushes are about 5 times thicker than the ones that have been reported so far.[35] At 25 °C a decrease in brush thickness was only observed after prolonged reaction times (18 h). These optimized reaction conditions were found to be very reproducible and have been used for all other NaMA polymerization experiments that are discussed below.

A question that is still unanswered is the origin of the observed increase in brush thickness with increasing monomer concentration, as illustrated in Figure 3. One obvious explanation could be screening of electrostatic repulsions due to the increased ionic strength of the reaction mixture at high monomer concentrations. To investigate this hypothesis, the kinetics of the SI-ATRP of a reaction mixture containing 100 mol equiv

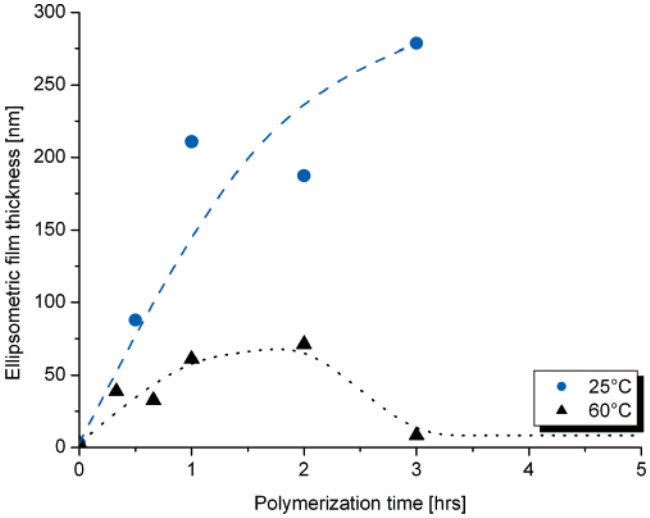

Figure 6. Effect of temperature on the kinetics of the SI-ATRP of NaMA using the reaction system: NaMA/CuBr/$CuBr_2$/bipy/water = 200:2:0.4:5:1400, pH = 9.

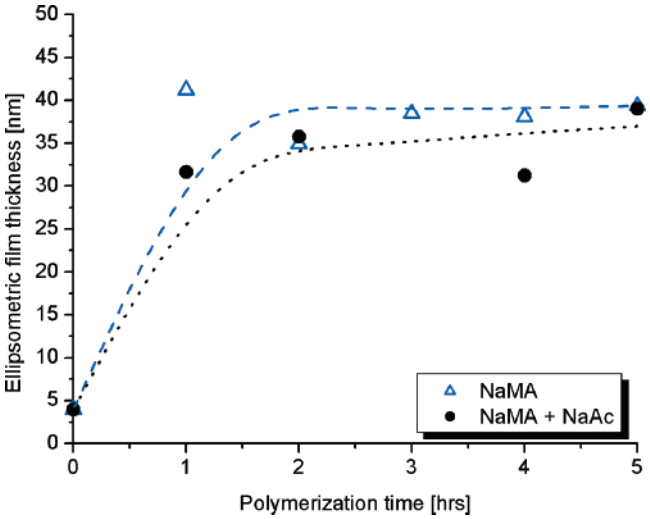

Figure 7. Effect of ionic strength on the SI-ATRP of NaMA at 25 °C and pH = 9. A reaction system containing 100 mol equiv of NaMA is compared to a system with 100 mol equiv of NaMA and 100 mol equiv of NaAc. Ratios of other components in the polymerization solution are kept constant at CuBr/$CuBr_2$/bipy/water = 2:0.4:5:1400.

NaMA were studied both in the absence and in the presence of 100 mol equiv of sodium acetate (NaAc) as an inert electrolyte (Figure 7). The data in Figure 7 clearly indicate that the growth kinetics of the PMAA brushes does not depend on the ionic strength of the polymerization medium. This suggests that the increase in film thickness that is shown in Figure 3 is due to the increase in monomer concentration. Comparison of the data presented in Figures 7 and 2 also underlines again the dramatic effect of the reaction temperature on the brush growth. At a monomer concentration of 100 mol equiv, SI-ATRP of NaMA at 60 °C resulted in a film thickness of 7 nm after 3 h, whereas PMAA brushes of 40 nm thickness were obtained after a polymerization time of 2 h at 25 °C.

The SI-ATRP methodology also allowed the preparation of poly(methacrylic acid)-*b*-poly(2-hydroxyethyl methacrylate) (PMAA-*b*-PHEMA) brushes using the PMAA brushes as macroinitiator for the polymerization of HEMA. Growth of the PHEMA block resulted in an increase in film thickness from 43 to 66 nm and was accompanied by a slight increase in the advancing water contact angle from 55° to 60° (Table 1). Further support for the successful chain extension is obtained from the

Table 1. Ellipsometric Film Thicknesses and Water Contact Angles of PMAA and PMAA-*b*-PHEMA Brushes[a]

brush	ellipsometric thickness [nm]	advancing water contact angle [deg]	receding water contact angle [deg]
PMAA	43	55 (Lit[35]: 56)	0 (Lit[35]: 0)
PMAA-*b*-PHEMA	66	60 (Lit(PHEMA)[43]: 60)	20

[a] The PMAA brush was prepared by SI-ATRP of NaMA for 15 min at 25 °C using a polymerization system consisting of NaMA/CuBr/$CuBr_2$/bipy/water in the following molar ratios: 200:2:0.4:5:1400. The PMAA-*b*-PHEMA brush was obtained by extending the PMAA brush via SI-ATRP of HEMA at 25 °C for 2.5 h using a reaction system composed of HEMA/CuCl/$CuBr_2$/bipy/water in the following molar ratios: 215:3.4:1:9.75:1430.

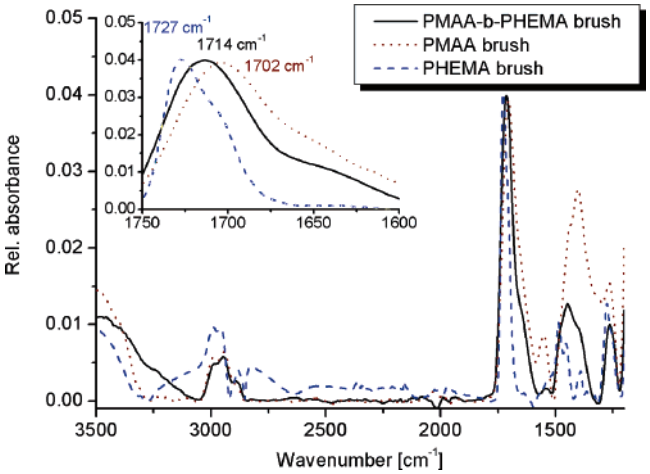

Figure 8. ATR-FTIR spectra of a 43 nm thick PMAA brush and a 66 nm thick PMAA-*b*-PHEMA diblock copolymer brush obtained by extension of the PMAA brush with HEMA. The spectrum of a ~100 nm thick PHEMA brush is shown as reference.

ATR-FTIR spectra shown in Figure 8. Whereas the FTIR spectrum of the PMAA brush reveals a carbonyl band at 1702 cm^{-1}, which is characteristic for hydrogen-bonded dimers of carboxylic acid groups,[38] the carbonyl band in the block copolymer brush is shifted to 1714 cm^{-1}. This shift is due to the superposition of the carbonyl band of the dimerized carboxylic acid groups and that of the ester carbonyl of the PHEMA block, which appears at 1727 cm^{-1}. Figure 9 compares the C_{1s} XPS high-resolution scans of a PMAA brush, the corresponding PMAA-*b*-PHEMA diblock copolymer brush, and a PHEMA brush. Figure 9 shows that the spectrum of the diblock copolymer brush can be regarded as a superposition of the two corresponding homopolymer brushes, which provides additional support for the successful extension of the PMAA brush with HEMA. Although detailed kinetic studies will be necessary to unequivocally demonstrate the living character of the SI-ATRP of NaMA, the ability to control brush thickness via polymerization time and the possibility to extend the PMAA brushes with a PHEMA block are characteristic features of controlled/"living" radical polymerizations.

Variation of Brush Density. All brushes that have been discussed so far were grown from silicon or glass surfaces modified with the ATRP initiator-functionalized trimethoxysilane **1**. The objective of the next series of experiments was to produce PMAA brushes with varying chain density. To control the chain density of the PMAA brushes, glass or silicon substrates were first modified with mixtures of the ATRP initiator-functionalized trimethoxysilane **1** and a structurally similar but "ATRP inactive" pivaloyl-functionalized trimethoxysilane **2**. The modification of the substrates was carried out at a constant total concentration of trimethoxysilane but with varying solution mole fractions of both components ($\chi_1^{solution}$ and $\chi_2^{solution}$, respectively). It was anticipated that variation of $\chi_1^{solution}$ would allow control of brush density.

To assess the feasibility of the mixed alkoxysilane-based initiator layers to control brush density, a series of six samples was prepared with $\chi_1^{solution} = 0$, 0.2, 0.4, 0.6, 0.8, and 1, respectively. The samples were subsequently analyzed with XPS to determine the surface mole fraction of **1** ($\chi_1^{surface}$). $\chi_1^{surface}$ was determined from high-resolution XPS Br_{3d} and N_{1s} scans (Figure 1). Because both alkoxysilane derivatives contain an amide bond, the N_{1s} signal was used as a reference. After correction of the Br_{3d} and N_{1s} signals with their respective relative sensitivity factors, $\chi_1^{surface}$ was estimated using the following equations: $\chi_1^{surface} = I/(I_0)$ (I), with $I = (I_{Br3d})/(I_{N1s}) = (A_{Br3d} \cdot RSF_{Br})/(A_{N1s} \cdot RSF_N)$ (II). In equation (I), I_0 is the intensity of an initiator layer that consists exclusively of **1**. In equation (II), A is the peak area, and RSF_{Br} and RSF_N are the relative sensitivity factors for bromine and nitrogen (5.479 and 2.681, respectively). Figure 10 compares $\chi_1^{surface}$ estimated using equations (I) and (II) with $\chi_1^{solution}$ and shows that it is possible to control the surface mole fraction of ATRP initiator groups via adjustment of the solution mole fractions. Figure 10, however, also very clearly shows that, in all cases, $\chi_1^{surface}$ is significantly lower than expected based on $\chi_1^{solution}$. Given the similarity in chemical structure between **1** and **2**, this seems quite surprising. The reasons for the discrepancy between $\chi_1^{surface}$ and $\chi_1^{solution}$ are not fully understood at the moment and are the subject of ongoing investigations. It is, however, interesting to note that qualitatively similar results were recently reported by Chilkoti et al., who compared the surface composition of self-assembled monolayers (SAMs) of ω-mercaptoundecyl bromoisobutyrate and undecanethiol with the mole fractions of both compositions in the solution that was used to prepare the SAMs.[44]

Silicon substrates modified with mixtures of **1** and **2** of different composition were subsequently used to grow PMAA brushes. SI-ATRP was carried out in a single large reaction vessel, which contained the complete series of substrates. The polymerization was performed using 200 mol equiv of monomer at pH 9 and 25 °C for 25 min. Figure 11 plots the ellipsometric thickness of the resulting brushes as a function of $\chi_1^{solution}$. SI-ATRP of NaMA from substrates modified with $\chi_1^{solution} < 0.5$ yielded only thin polymer brushes with a thickness of ~7 nm. A strong increase in brush thickness was observed for $\chi_1^{solution} > 0.5-0.7$, which marks the transition from the mushroom to the brush regime. At this point, steric repulsions between neighboring PMAA chains induce stretching of the polymer backbone. It is interesting to note that Figure 11 is in good qualitative agreement with the results that are presented in Figure 10. Figure 11 indicates that the crossover from the mushroom to the brush regime only occurs at relatively high values for $\chi_1^{solution}$. This observation is in good agreement with the findings from Figure 10, which show that the surface mole fraction of ATRP initiator **1** in mixed alkoxysilane initiator layers is always lower than that predicted based on the solution mole fractions.

Mineralization of Calcium Carbonate. Next, the PMAA brushes were investigated as substrates for the mineralization of calcium carbonate. To this end, PMAA brushes grown from glass slides modified using $\chi_1^{solution} = 0.3$, 0.6, 0.8, and 1.0 were placed in a perfusion cell and subjected to a continuous flow of a supersaturated $CaCO_3$ solution. After 30 min, the samples were taken from the perfusion cell, washed, dried, and inspected with differential interference microscopy. Interestingly, the

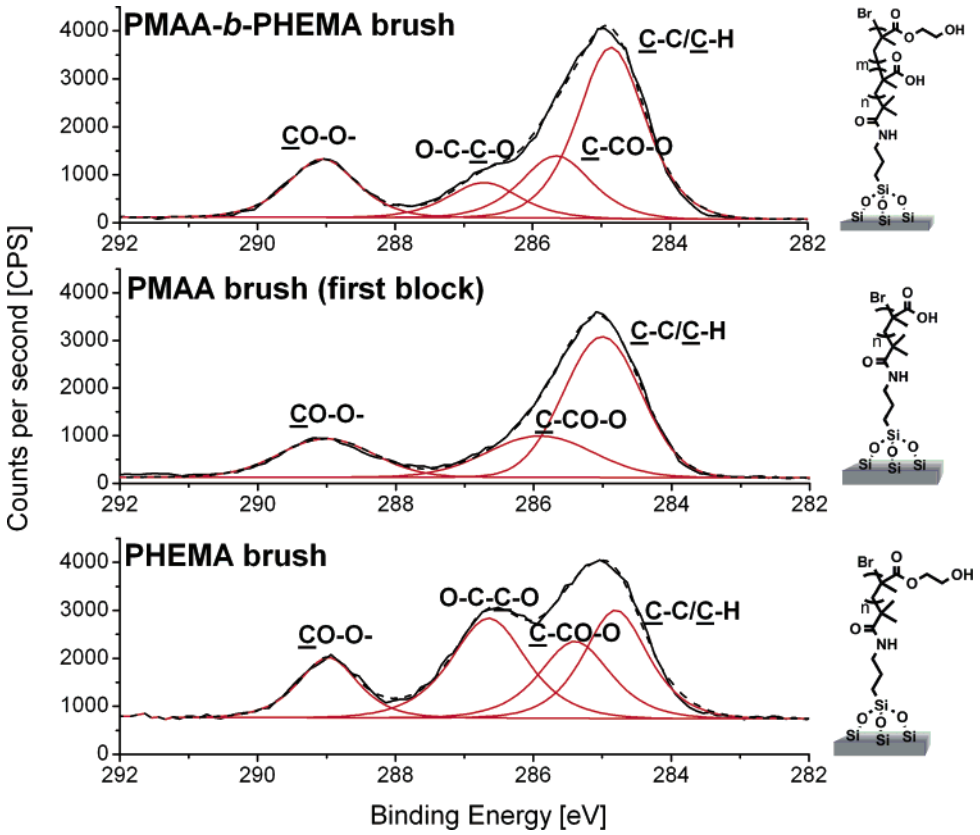

Figure 9. High-resolution XPS spectra of the C_{1s} signals of a 66 nm thick PMAA-*b*-PHEMA brush, a 43 nm thick PMAA brush, and a ~100 nm thick PHEMA brush.

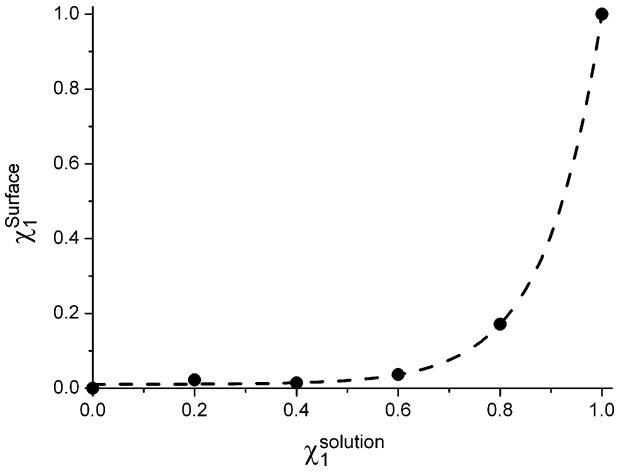

Figure 10. Surface mole fraction of ATRP initiator **1** ($\chi_1^{surface}$) as a function of its mole fraction in the reaction mixture ($\chi_1^{solution}$) that is used for the modification of the silicon substrates.

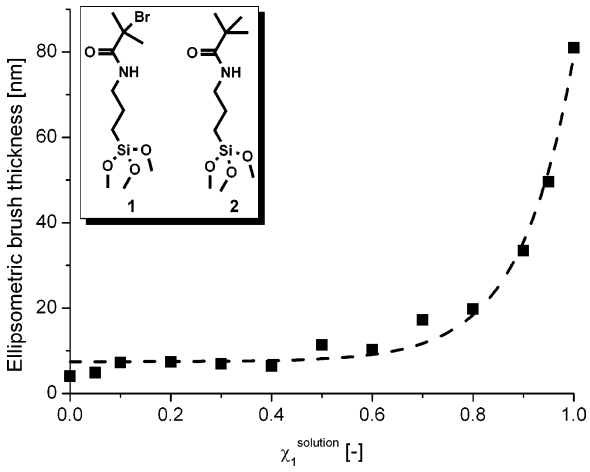

Figure 11. Ellipsometric thicknesses of PMAA brushes grown by SI-ATRP of NaMA as a function of $\chi_1^{solution}$ that was used to prepare the initiator-functionalized silicon substrates. Polymerizations were carried out at 25 °C and pH 9 for 30 min using the following polymerization conditions: NaMA/CuBr/$CuBr_2$/bipy/water = 200:2:0.4:5:1400.

images in Figure 12 reveal that, whereas PMAA brushes generated from surfaces modified with $\chi_1^{solution} = 0.3$ or 0.6 resulted in the formation of randomly oriented calcite crystals showing the typical rhombohedral crystal habit, brushes obtained from surfaces functionalized with $\chi_1^{solution} = 1.0$ completely prevented crystallization and induced the deposition of a layer of amorphous $CaCO_3$ (ACC). On PMAA brushes prepared from surfaces modified with $\chi_1^{solution} = 0.8$, both the formation of calcite crystals as well as the deposition of ACC was observed. The ability of the PMAA brushes to prevent $CaCO_3$ crystallization and allow the deposition of ACC is of technological interest because ACC can serve as a transient metastable precursor for the different crystal polymorphs of calcium carbonate.[45−47]

It is interesting to compare the mineralization behavior of $CaCO_3$ with the wetting properties of the PMAA brushes. Figure 13 shows the advancing and receding water contact angles both on pristine PMAA brushes as well as on PMAA brushes that were incubated with a 10 mM $CaCl_2$ solution prior to the contact angle measurements. Figure 13 indicates a significant drop in the receding water contact angle on PMAA brushes grown from surfaces modified with $\chi_1^{solution} > 0.6$, especially after incubation with $CaCl_2$. A similar drop was also observed in the advancing water contact angle on brushes incubated in $CaCl_2$. The decrease in advancing water contact angle upon incubation with Ca^{2+} is reminiscent of earlier observations by Huck et al. and suggests

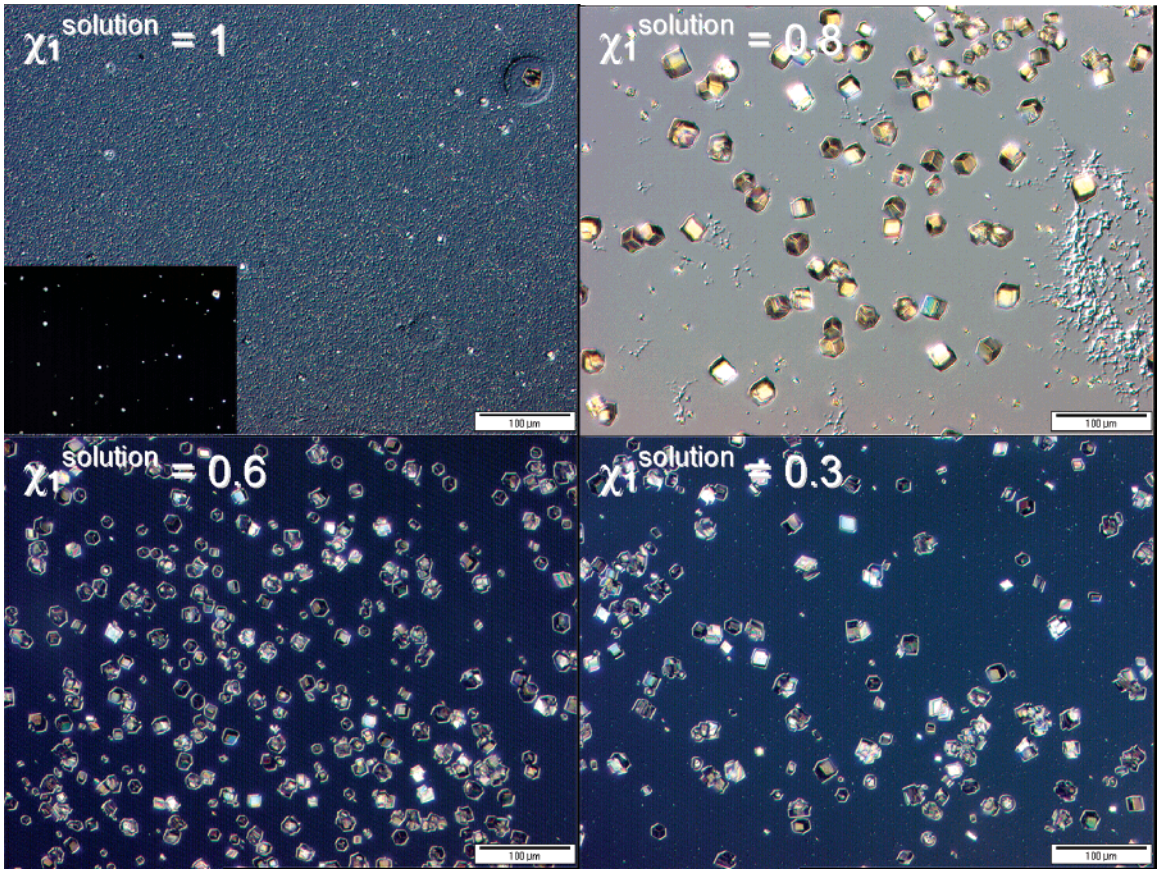

Figure 12. Differential interference contrast (DIC) micrographs of mineralized PMAA brushes of varying grafting density. The insert in the image of the brush generated from a surface modified with $\chi_1^{solution} = 1.0$ was taken between crossed polarizers and illustrates the amorphous nature of the deposited $CaCO_3$ layer.

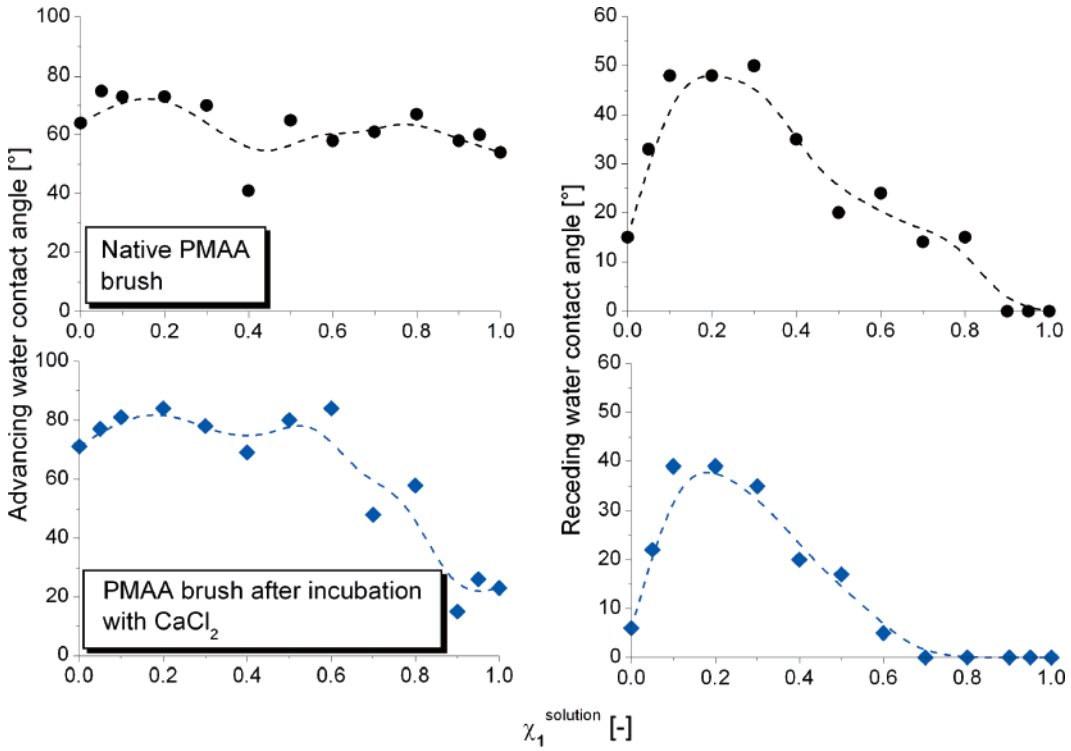

Figure 13. Advancing and receding water contact angles on PMAA brushes with varying grafting densities before and after incubation with aqueous 10 mM $CaCl_2$ solution. Polymerizations were carried out at 25 °C and pH 9 for 30 min using the following polymerization conditions: NaMA/CuBr/$CuBr_2$/bipy/water = 200:2:0.4:5:1400.

a collapse of the PMAA brush.[17] Although the collapsed PMAA brushes will contain less water than their fully hydrated analogues, they will contain a significant amount of hydrated electrolyte that results in the observed hydrophilic surfaces properties. It is interesting to note that the dramatic change in wetting properties of the $CaCl_2$ incubated PMAA brushes

prepared from surfaces modified with $\chi_1^{solution} > 0.6$ coincides with the changes in the $CaCO_3$ crystallization behavior illustrated in Figure 12. Upon comparison of the results shown in Figures 10−13, it is tempting to propose a correlation between the conformation of the tethered PMAA chains and the wetting and mineralization properties of the polymer brushes. Low-density brushes, which are in the mushroom regime, induce the deposition of calcite crystals, whereas high-density brushes, which are completely wetted, lead to the deposition of ACC. The results provided here, however, are not sufficient to unequivocally prove this hypothesis, and additional experiments are needed to establish a clear relationship between brush density, brush conformation, and calcium carbonate mineralization. This is the subject of ongoing investigations.

Conclusions

In the first part of this paper, the influence of different reaction parameters on the SI-ATRP of NaMA was investigated. In particular, reaction temperature and monomer concentration were identified as important parameters that strongly influence the growth of the brushes. A protocol has been developed that allows the preparation of PMAA brushes of up to 300 nm thickness via room-temperature, aqueous SI-ATRP of NaMA. The PMAA brushes could be used to initiate the ATRP of HEMA, which resulted in the formation of PMAA-*b*-PHEMA diblock copolymer brushes. In the second part of the paper, it was shown that the chain density of the PMAA brushes could be varied by modifying the SiO_x substrates with mixtures containing different relative amounts of an ATRP initiator-functionalized trimethoxysilane and an ATRP inactive trimethoxysilane. In spite of the similarity in chemical structure, however, XPS studies revealed that the surface molar ratio of the ATRP initiator-functionalized trimethoxysilane was always lower than expected based on its mole fraction in the reaction mixture that was used to modify the substrate. Finally, the feasibility of the PMAA brushes to direct the crystallization of $CaCO_3$ was investigated. To this end, a series of PMAA brushes of varying chain density was exposed to a supersaturated $CaCO_3$ solution. Interestingly, the formation of calcite crystals was observed on low-density PMAA brushes, while an amorphous film of $CaCO_3$ was deposited on PMAA brushes of high chain density. Because amorphous $CaCO_3$ can serve as a transient metastable precursor for different crystalline polymorphs of $CaCO_3$, the PMAA brushes may be attractive templates for the bottom-up fabrication of nanostructure calcite layers with interesting photonic properties.[48,49] Detailed studies on the stabilization of amorphous $CaCO_3$ on high-density PMAA brushes and the subsequent formation of single-crystal calcite films have been reported elsewhere.[50]

Acknowledgment. This work was financially supported by the VolkswagenStiftung and the Swiss Innovation Promotion Agency (CTI, contract no. 7241.1 NMPP-NM, H.-A.K.) as well as the Deutsche Forschungsgemeinschaft (DFG priority program 1117 "principles of biomineralization", Vo 829/2-3, D.V.). We are grateful to Profs. N. Spencer and M. Textor (Laboratory for Surface Science and Technology, ETHZ, Zürich, Switzerland) and N. Xanthopoulos (Laboratoire de Métallurgie Chimique, EPFL, Lausanne, Switzerland) for their support with the XPS experiments.

References and Notes

(1) Edmondson, S.; Osborne, V. L.; Huck, W. T. S. *Chem. Soc. Rev.* **2004**, *33*, 14−22.
(2) Rühe, J.; Knoll, W. *J. Macromol. Sci., Polym. Rev.* **2002**, *C42*, 91−138.
(3) Zhao, B.; Brittain, W. J. *Prog. Polym. Sci.* **2000**, *25*, 677−710.
(4) Pyun, J.; Kowalewski, T.; Matyjaszewski, K. *Macromol. Rapid. Commun.* **2003**, *24*, 1043−1059.
(5) Ma, H.; Hyun, J.; Stiller, P.; Chilkoti, A. *Adv. Mater.* **2004**, *16*, 338−341.
(6) Tugulu, S.; Arnold, A.; Sielaff, I.; Johnsson, K.; Klok, H.-A. *Biomacromolecules* **2005**, *6*, 1602−1607.
(7) Brown, A. A.; Khan, N. S.; Steinbock, L.; Huck, W. T. S. *Eur. Polym. J.* **2005**, *41*, 1757−1765.
(8) Xu, F. J.; Zhong, S. P.; Yung, L. Y. L.; Kang, E. T.; Neoh, K. G. *Biomacromolecules* **2004**, *5*, 2392−2403.
(9) Huber, D. L.; Manginell, R. P.; Samara, M. A.; Kim, B.-I.; Bunker, B. C. *Science* **2003**, *301*, 352−354.
(10) Boyes, S. G.; Akgun, B.; Brittain, W. J.; Foster, M. D. *Macromolecules* **2003**, *36*, 9539−9548.
(11) Kim, D. J.; Lee, K.-B.; Lee, T. G.; Shon, H. K.; Kim, W.-J.; Paik, H-j.; Choi, I. S. *Small* **2005**, *1*, 992−996.
(12) Moro, T.; Takatori, Y.; Ishihara, K.; Konno, T.; Takigawa, Y.; Matsushita, T.; Chung, U.-I.; Nakamura, K.; Kawaguchi, H. *Nat. Mater.* **2004**, *3*, 829−836.
(13) Seidel, C. *Macromolecules* **2003**, *36*, 2536−2543.
(14) Mercurieva, A. A.; Birshtein, T. M.; Zhulina, E. B.; Iakovlev, P.; van Male, J.; Leermakers, F. A. M. *Macromolecules* **2002**, *35*, 4739−4752.
(15) Zhulina, E. B.; Klein Wolterink, J.; Borisov, O. V. *Macromolecules* **2000**, *33*, 4945−4953.
(16) Rühe, J.; Ballauff, M.; Biesalski, M.; Dziezok, P.; Gröhn, F.; Johannsmann, D.; Houbenov, N.; Hugenberg, N.; Konradi, R.; Minko, S.; Motornov, M.; Netz, R. R.; Schmidt, M.; Seidel, C.; Stamm, M.; Stephan, T.; Usov, D.; Zhang, H. *Adv. Polym. Sci.* **2004**, *165*, 79−150.
(17) Moya, S.; Azzaroni, O.; Farhan, T.; Osborne, V. L.; Huck, W. T. S. *Angew. Chem., Int. Ed.* **2005**, *44*, 4578−4581.
(18) Addadi, L.; Weiner, S. *Proc. Natl. Acad. Sci. U.S.A.* **1985**, *82*, 4110−4114.
(19) Douglas, T. *Science* **2003**, *299*, 1192−1193.
(20) Aizenberg, J.; Black, A. J.; Whitesides, G. M. *Nature* **1999**, *398*, 495−498.
(21) Aizenberg, J.; Muller, D. A.; Grazul, J. L.; Hamann, D. R. *Science* **2003**, *299*, 1205−1208.
(22) Mann, S.; Heywood, B. R.; Rajam, S.; Walker, J. B. A.; Davey, R. J.; Birchall, J. D. *Adv. Mater.* **1990**, *2*, 257−261.
(23) Berman, A.; Ahn, D. J.; Lio, A.; Salmeron, M.; Reichert, A.; Charych, D. *Science* **1995**, *269*, 515−518.
(24) Wada, N.; Suda, S.; Kanamura, K.; Umegaki, T. *J. Colloid Interface Sci.* **2004**, *279*, 167−174.
(25) Hosoda, N.; Sugawara, A.; Kato, T. *Macromolecules* **2003**, *36*, 6449−6452.
(26) Tanaka, Y.; Nemoto, T.; Naka, K.; Chujo, Y. *Polym. Bull.* **2000**, *45*, 447−450.
(27) Falini, G.; Fermani, S.; Gazzano, M.; Ripamonti, A. *Chem.—Eur. J.* **1998**, *4*, 1048−1052.
(28) Archibald, D. D.; Qadri, S. B.; Gaber, B. P. *Langmuir* **1996**, *12*, 538−546.
(29) Patten, T. E.; Matyjaszewski, K. *Adv. Mater.* **1998**, *10*, 901−915.
(30) Sankhe, A. Y.; Husson, S. M.; Kilbey, S. M., II. *Macromolecules* **2006**, *39*, 1376−1383.
(31) Matyjaszewski, K.; Miller, P. J.; Shukla, N.; Immaraporn, B.; Gelman, A.; Luokala, B. B.; Siclovan, T. M.; Kickelbick, G.; Vallant, T.; Hoffmann, H.; Pakula, T. *Macromolecules* **1999**, *32*, 8716−8724.
(32) Treat, N. D.; Ayres, N.; Boyes, S. G.; Brittain, W. J. *Macromolecules* **2006**, *39*, 26−29.
(33) Wu, T.; Genzer, J.; Gong, P.; Szleifer, I.; Vlček, P.; Šubr, V. In *Polymer Brushes: Synthesis, Characterization, Applications*; Advincula, R. C., Brittain, W. J., Caster, K. C., Rühe, J., Eds.; Wiley: Weinheim, **2004**; Chapter 15.
(34) Ashford, E. J.; Naldi, V.; O'Dell, R.; Billingham, N. C.; Armes, S. P. *Chem. Commun.* **1999**, 1285−1286
(35) Osborne, V. L.; Jones, D. M.; Huck, W. T. S. *Chem. Commun.* **2002**, 1838−1839.
(36) Scofield, J. H. *J. Electron Spectrosc. Relat. Phenom.* **1976**, *8*, 129−137.
(37) Volkmer, D.; Harms, M.; Gower, L.; Ziegler, A. *Angew. Chem., Int. Ed.* **2005**, *44*, 639−644.
(38) Niwa, M.; Mori, T; Higashi, N. *Macromolecules* **1995**, *28*, 7770−7774.
(39) Beyer, M. K.; Clausen-Schaumann, H. *Chem. Rev.* **2005**, *105*, 2921−2948.
(40) Tugulu, S.; Klok, H.-A., unpublished results.
(41) Wasserman, S. R.; Tao, Y. -T.; Whitesides, G. M. *Langmuir* **1989**, *5*, 1074−1087.

(42) Onclin, S.; Ravoo, B. J.; Reinhoudt, D. N. *Angew. Chem., Int. Ed.* **2005**, *44*, 6282−6304.
(43) Jones, D. M.; Huck, W. T. S. *Adv. Mater.* **2001**, *13*, 1256−1259.
(44) Ma, H.; Wells, M.; Beebe, T. P.; Chilkoti, A. *Adv. Funct. Mater.* **2006**, *16*, 640−648.
(45) Koga, N.; Nakagoe, Y.; Tanaka, H. *Thermochim. Acta* **1998**, *318*, 239−244.
(46) Raz, S.; Weiner, S.; Addadi, L. *Adv. Mater.* **2000**, *12*, 38−42.
(47) Loste, E.; Meldrum, F. C. *Chem. Commun.* **2001**, 901−902.
(48) Parker, A. R.; McPhedran, R. C.; McKenzie, D. R.; Botten, L. C.; Nicorovici, N.-A. P. *Nature* **2001**, *409*, 36−37.
(49) Zakhidov, A. A.; Baughman, R. H.; Iqbal, Z.; Cui, C.; Khayrullin, I.; Dantas, S. O.; Marti, J.; Ralchenko, V. G. *Science* **1998**, *282*, 897−901.
(50) Tugulu, S.; Harms, M.; Fricke, M.; Volkmer, D.; Klok, H.-A. *Angew. Chem. Int. Ed.* **2006**, *45*, 7458−7461.

MA060739E